Time-Resolved Optical Gating Based on Dispersive Propagation: A New Method to Characterize Optical Pulses

Roger G. M. P. Koumans and Amnon Yariv, *Life Fellow, IEEE*

***Abstract*—We introduce the technique of time-resolved optical gating (TROG) based on dispersive propagation (DP), a new noninterferometric method for characterizing ultrashort optical pulses in amplitude and phase without the need for a short optical gating pulse. TROG is similar to frequency-resolved optical gating except that the role of time and frequency is interchanged. For the DP-TROG geometry, we show that measurements of the autocorrelation trace of the pulse after propagation through a medium with variable dispersion together with a single measurement of its intensity spectrum contain sufficient information to reconstruct the pulse in amplitude and phase. Pulse reconstruction for this DP-TROG geometry works very well even for the case of a nonlinearly chirped double pulse. Compared with other methods, DP-TROG does not introduce an ambiguity in the direction of time for the pulse. Due to its simplicity and improved sensitivity, DP-TROG is expected to be useful in characterizing low-energy pulses.**

***Index Terms*—Optical correlators, optical fiber dispersion, optical propagation in dispersive media, optical pulse compression, optical pulse measurements, pulse characterization, time-domain measurements.**

I. Introduction

THE NUMBER of methods to characterize optical pulses has increased extensively over the last decade. The most popular method is to measure its intensity (or background-free) autocorrelation trace by mixing the pulse with a delayed version of itself in a second-harmonic generating (SHG) crystal [1], [2]. Temporal decorrelation of the intensity autocorrelation trace of a laser pulse has recently been demonstrated theoretically [3], but the method does not always reconstruct the intensity of the pulse correctly. An often-used variant to the measurement of the background-free autocorrelation trace is the measurement of the interferometric (or fringe-resolved) autocorrelation trace [4]. However, complete reconstruction of the phase and amplitude of the pulse is complicated: an accurate measurement of the fringes is needed and a careful deconvolution method has to be used [5], [6]. Besides these time-domain methods, a number of frequency-domain methods have been used as well. A frequency-domain interferometric method called spectral phase interferometry for direct electric-field reconstruction (SPIDER) has recently been introduced by Iaconis and Walmsley [7] and allows for pulse reconstruction without an iterative algorithm.

A number of noninterferometric pulse characterization methods are available as well besides the interferometric methods. A very powerful method to characterize optical pulses—frequency-resolved optical gating (FROG)—has been introduced by Kane and Trebino [8]–[13]. In this method, the pulse to be characterized is cross-correlated with a delayed gating pulse in a nonlinear crystal to generate a higher harmonic light output. The spectrum of this higher harmonic is measured as a function of the delay of the gating pulse. The gating pulse can take on many shapes depending on the measurement setup (also called geometry) that is used [14]. The measured spectra make up a two-dimensional (2-D) FROG trace. The amplitude and phase of the pulse can be reconstructed from this measured FROG trace by an iterative algorithm based on generalized projections (GP) [15]–[18]. The GP method has recently been improved and the resulting principal component generalized projections algorithm (PCGPA) [19] is fast enough to allow real-time inversion of FROG spectrograms [20].

Another time-domain noninterferometric characterization method—frequency-domain phase measurement (FDPM)—was proposed by Chilla and Martinez [21]–[23]. In this method, a spectral slice of the pulse is selected by a grating and a slit and this slice is cross-correlated with the original pulse in a SHG crystal. Cross-correlation traces are then measured for different spectral slices of the pulse. This method is similar to the FROG method described above except that the role of frequency and time are interchanged: the gating takes place in the frequency domain and cross-correlation traces are measured instead of spectra. The actual measurements are resolved in the time domain and it would, therefore, be appropriate to put this method in a more general category which we will call time-resolved optical gating (TROG). FDPM can then be seen as a measurement setup or geometry for TROG. For the FDPM geometry, the measured traces make up a 2-D TROG trace from which the phase and amplitude of the pulse can be retrieved using a similar iterative algorithm as the one that is used for FROG [24].

Although various measurement geometries have been explored for FROG, the number of geometries available for TROG is limited. The available geometries are based on cross-correlating a spectrally filtered version of the pulse with a short gating pulse which usually is the original unfiltered pulse or a known reference pulse. In this paper, we propose a new TROG geometry based on dispersive propagation (DP-TROG) which

Manuscript received January 1, 1999; revised June 29, 1999. This work was supported by the Defense Advanced Research Projects Agency (DARPA, R. Leheny) and by the Office of Naval Research (ONR, Y. S. Park).

The authors are with the Department of Applied Physics, California Institute of Technology, Pasadena, CA 91125 USA.

Publisher Item Identifier S 0018-9197(00)00959-3.

does not have the short gate requirement. In this technique, the spectrally filtered pulse is autocorrelated in a SHG crystal instead of cross-correlated with a short gating pulse. It will be shown that a single measurement of the intensity spectrum of the pulse together with measurements of its autocorrelation trace after propagation through a medium with variable dispersion provide enough information to reconstruct the phase and amplitude of the pulse using an iterative algorithm.

This paper is divided in the following way. Section II deals with the basics and notational concepts of TROG. Section III will describe the DP-TROG geometry in detail and prove that the data provided by a DP-TROG trace is sufficient for a complete determination of the pulse in amplitude and phase. Section IV will describe briefly the specifics of the reconstruction algorithm and show how well the method works for the case of a nonlinearly chirped double pulse. Section V summarizes the DP-TROG method and discusses the differences with other methods.

II. Basics of TROG

The electric field representing an ultrashort optical pulse can be described in the time domain as

$$E(t) = A(t)\exp(+j2\pi f_0 t) \tag{1}$$

where f_0 is the carrier frequency and $A(t)$ is the slowly varying complex envelope of the field representing the amplitude and phase of the pulse. $A(t)$ is normalized in such a way that $|A(t)|^2$ represents the intensity of the pulse. One can also represent the electric field in the frequency domain by Fourier transforming it as

$$\tilde{E}(f) = \tilde{A}(f - f_0) \tag{2}$$

where $\tilde{E}(f)$ is the Fourier transform of $E(t)$ and $\tilde{A}(f)$ is the Fourier transform of $A(t)$. Throughout this paper, the following Fourier transform pairs are used:

$$\tilde{X}(f) = \int X(t)\exp(-j2\pi f t)\,dt \tag{3a}$$

$$X(t) = \int \tilde{X}(f)\exp(+j2\pi f t)\,df \tag{3b}$$

and all integrals in this paper are assumed to be from $-\infty$ to $+\infty$.

We will now introduce the basics of TROG and show how FDPM can be considered as a TROG geometry. A schematic diagram for the measurement of a TROG trace is shown in Fig. 1. The spectrum of the pulse $\tilde{A}(f)$ is spectrally filtered in the frequency domain with a filter function $\tilde{H}_{\mathrm{TROG}}(f, F)$, giving the signal field

$$\tilde{S}_{\mathrm{TROG}}(f, F) = \tilde{A}(f)\tilde{H}_{\mathrm{TROG}}(f, F). \tag{3}$$

The signal field is next filtered in the time domain and detected by an integrating square-law detector. The signal at the output of the detector is given by

$$I_{\mathrm{TROG}}(T, F) = \int |G_{\mathrm{TROG}}(t, T)|^2 \cdot \left| \int \tilde{A}(f)\tilde{H}_{\mathrm{TROG}}(f, F)\exp(j2\pi f t)\,df \right|^2 dt. \tag{4}$$

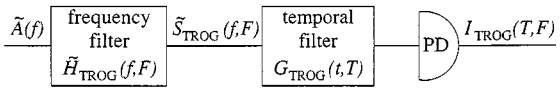

Fig. 1. Schematic diagram for the TROG measurement setup consisting of a frequency gate followed by a temporal filter and an integrating photodetector (PD).

This quantity is called the TROG trace or sonogram of the input pulse; it measures the temporal intensity of different spectral components of the pulse. It is noted that TROG has a time–frequency duality with FROG where the spectral intensity of different temporal components of the pulse is measured.

The FDPM method introduced by Chilla and Martinez can be considered a TROG geometry. Although its name might imply that it is a frequency-resolved measurement, the measurement is resolved in time as a number of cross-correlation traces is measured instead of spectra. From now on, we will refer to FDPM as FDPM-TROG. In the experiment of Chilla and Martinez [21], the spectral filtering is performed by a grating and a slit. An exact transfer function of this grating/slit pair, taking into account the spatial variation of the optical beam, is given in [22]. For a slit size larger than the beam size, this transfer function can be simplified to a rectangle function

$$\tilde{H}_{\mathrm{FDPM-TROG}}(f, F) = \begin{cases} 1, & \text{for } |f - F| \le \frac{1}{2}F_0 \\ 0, & \text{for } |f - F| > \frac{1}{2}F_0 \end{cases} \tag{5}$$

where F_0 is the frequency passband of the slit. The pulse at the output of the slit is cross-correlated with the original pulse in a SHG crystal. If the width of the slit is small enough so that the duration of the resulting pulse is much longer than the original pulse, the temporal transfer function will approach a delta-function, $|G_{\mathrm{FDPM-TROG}}(t, T)|^2 \rightarrow \delta(t - T)$, and the detected signal is given by

$$I_{\mathrm{FDPM-TROG}}(T, F) = \left| \int \tilde{A}(f)\tilde{H}_{\mathrm{FDPM-TROG}}(f, F)\cdot\exp(j2\pi f T)\,df \right|^2. \tag{6}$$

Although Chilla and Martinez state that better spectral resolution and phase reconstruction is obtained with a narrower slit, Wong and Walmsley show that this is not necessary if the pulse reconstruction algorithm uses the entire detected signal of (6) instead of just the temporal locations of the centers of the cross-correlation traces [24].

A diagram of the pulse reconstruction algorithm for TROG is shown in Fig. 2. The algorithm is started from an initial random guess for the complex spectrum of the pulse $\tilde{A}^{(0)}(f)$. On the kth iteration, the signal field $\tilde{S}^{(k)}_{\mathrm{TROG}}(f, F)$ is calculated according to (3) from $\tilde{A}^{(k)}(f)$. It is next inverse Fourier transformed with respect to f to give $S^{(k)}_{\mathrm{TROG}}(T, F)$. At this point, the time-domain constraint is applied, giving a new signal field

$$S'_{\mathrm{TROG}}(T, F) = \sqrt{I_{\mathrm{TROG}}(T, F)}\,\frac{S^{(k)}_{\mathrm{TROG}}(T, F)}{|S^{(k)}_{\mathrm{TROG}}(T, F)|} \tag{7}$$

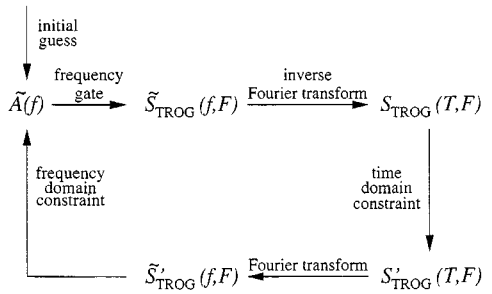

Fig. 2. Diagram of the pulse reconstruction algorithm for TROG.

by replacing the magnitude of the signal field $S^{(k)}_{\mathrm{TROG}}(T, F)$ by the square root of the measured TROG trace $I_{\mathrm{TROG}}(T, F)$. This signal field is then Fourier transformed with respect to T to give the signal function $\tilde{S}'_{\mathrm{TROG}}(f, F)$. The frequency-domain constraint is next applied to give a new guess for the pulse envelope $\tilde{A}^{(k+1)}(f)$ by minimizing the signal field error defined by

$$\hat{\epsilon}^{(k)}_{\mathrm{TROG}} = \sigma(\tilde{S}'_{\mathrm{TROG}}(f_i, F_j), \tilde{A}^{(k+1)}(f_i)\tilde{H}^{(k+1)}_{\mathrm{TROG}}(f_i, F_j)) \tag{8}$$

with respect to $\tilde{A}^{(k+1)}(f_i)$, where the rms error is defined by

$$\sigma(X_{ij}, Y_{ij}) = \left\{ \frac{1}{N^2} \sum_{j=1}^{N} \sum_{i=1}^{N} |X_{ij} - Y_{ij}|^2 \right\}^{1/2}. \tag{9}$$

It is noted that $\tilde{H}^{(k+1)}_{\mathrm{TROG}}(f_i, F_j)$ can depend on $\tilde{A}^{(k+1)}(f_i)$ implicitly. This process is iterated until convergence is reached. We have assumed here that the measured TROG trace is given on a $N \times N$ grid, where the frequency separation between two frequency points equals $\Delta F = F_{n+1} - F_n$.

A good criterion for the convergence of the algorithm is given by the error between the measured and reconstructed TROG trace

$$\epsilon^{(k)}_{\mathrm{TROG}} = \sigma(I_{\mathrm{TROG}}(T_i, F_j), \alpha^{(k)}|S^{(k)}_{\mathrm{TROG}}(T_i, F_j)|^2) \tag{10}$$

where $\alpha^{(k)}$ is a scaling parameter that minimizes the error on each iteration [13]. We note that the frequency separation between two time points $\Delta T = T_{n+1} - T_n$ is related to ΔF by

$$\Delta T = \frac{1}{N\Delta F}. \tag{11}$$

An error ϵ_{TROG} on the order of 10^{-3} or smaller usually indicates good pulse reconstruction.

III. Dispersive Propagation (DP): A New TROG Geometry

We propose a new measurement setup for TROG that makes use of DP. A schematic diagram of the DP-TROG geometry is pictured in Fig. 3. The setup consists of a phase stationary filter (the disperser) followed by an amplitude nonstationary filter (the autocorrelator) and a square-law integrating detector. Variable DP can, for example, be accomplished by a grating pair disperser [25], a set of prisms [26], or a number of normal/anomalous dispersive fibers each with a different length.

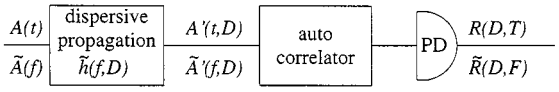

Fig. 3. Schematic measurement setup for DP-TROG consisting of a disperser followed by an autocorrelator and an integrating photodetector (PD).

Without loss of generality, we will consider the case where the DP takes place in a set of fibers, each with a different amount of dispersion. The spectral transfer function for a piece of dispersive fiber is given by [1]

$$\tilde{h}(f, D) = \exp(j\pi f^2 D) \tag{12}$$

where $D = -2\pi\beta_2 L$ is the total dispersion of the fiber with length L and with a dispersion parameter β_2 that is negative for regular fiber and positive for dispersion-compensating fiber. The detected signal at the output of the intensity autocorrelator is given by [1], [2]

$$R(D, T) = \int |A'(t, D)|^2 |A'(t - T, D)|^2 \, dt \tag{13}$$

where $A'(t, D)$ is the pulse envelope after DP through a fiber with total dispersion D. The Fourier transform of $R(D, T)$ with respect to T can be written as

$$\tilde{R}(D, F) = \left| \int |A'(t, D)|^2 \exp(-j2\pi F t) \, dt \right|^2. \tag{14}$$

Using the convolution theorem for Fourier transforms, this can be rewritten as

$$\begin{aligned} \tilde{R}(D, F) &= \left| \int \tilde{A}'(f, D)\tilde{A}'^*(f - F, D) \, df \right|^2 \\ &= \left| \int \tilde{A}(f)\tilde{A}^*(f - F) \exp(j2\pi f F D) \, df \right|^2 \end{aligned} \tag{15}$$

where we have used

$$\tilde{A}'(f, D) = \tilde{A}(f)\tilde{h}(f, D) = \tilde{A}(f) \exp(j\pi f^2 D). \tag{16}$$

Comparing (15) with (6), we see that the Fourier transform of the measured trace $\tilde{R}(F, D)$ is a scaled version of the DP-TROG trace defined by

$$\begin{aligned} &I_{\mathrm{DP-TROG}}(T, F) \\ &\quad = \left| \int \tilde{A}(f)\tilde{H}_{\mathrm{DP-TROG}}(f, F) \cdot \exp(j2\pi f T) \, df \right|^2. \end{aligned} \tag{17}$$

For

$$\tilde{H}_{\mathrm{DP-TROG}}(f, F) = \tilde{A}^*(f - F) \tag{18}$$

and $T = FD$, the scaling is given by

$$I_{\mathrm{DP-TROG}}(T, F) = \tilde{R}(T/F, F). \tag{19}$$

The DP-TROG trace can thus be constructed from the measured set of autocorrelation traces $R(D, T)$ by Fourier transforming them with respect to T to give $\tilde{R}(D, F)$ and next interpolating this trace at points $(T_i/F_j, F_j)$ such that ΔT and ΔF are related by (11).

It is noted that interpolation of the trace with $F = 0$

$$I_{\mathrm{DP-TROG}}(T, 0) = \left| \int |\tilde{A}(f)|^2 \exp(j2\pi f T)\, df \right|^2 \tag{20}$$

is not possible. From (20), however, it can easily be seen that this trace is obtained by measuring the intensity spectrum $|\tilde{A}(f)|^2$ of the original pulse, inverse Fourier transforming it with respect to f, and finally squaring it in magnitude.

The pulse shape can next be retrieved from the TROG trace of (19) by the iterative TROG algorithm depicted in Fig. 2. It can thus be concluded that measurement of the autocorrelation traces of dispersed versions of the original pulse together with the spectrum of the original pulse provide enough information to reconstruct the pulse in amplitude and phase.

IV. DP-TROG Pulse Reconstruction

To demonstrate how well the pulse reconstruction works for this new DP-TROG method, we will use a nonlinearly chirped double pulse in our simulations. The pulse can be represented mathematically by

$$A(t) = |A(t)| \exp\{j\varphi(t)\} \tag{21}$$

where

$$|A(t)| = \exp\left\{-a\left(\frac{t-d}{t_0}\right)^2\right\} + b\exp\left\{-c\left(\frac{t-e}{t_0}\right)^2\right\} \tag{22}$$

and

$$\varphi(t) = \alpha\left(\frac{t}{t_0}\right) + \beta\left(\frac{t}{t_0}\right)^2 + \gamma\left(\frac{t}{t_0}\right)^3 + \delta\left(\frac{t}{t_0}\right)^4 + \varepsilon\left(\frac{t}{t_0}\right)^5. \tag{23}$$

The pulse parameters are chosen to be

$$\begin{aligned} &a = 0.75 \quad t_0 = 1\mathrm{ps} \\ &b = 0.50 \quad d = -1.0t_0 \\ &c = 2.00 \quad e = 2.0t_0 \end{aligned} \qquad \begin{aligned} \alpha &= -0.058 \\ \beta &= -0.41 \\ \gamma &= -0.000\,44 \\ \delta &= -0.0007 \\ \varepsilon &= -0.000\,03. \end{aligned} \tag{24}$$

The amplitude parameters have been chosen to obtain a double pulse in the time domain and the chirp parameters are taken from [8], except for the fact that β has been adapted to obtain a double-peaked intensity spectrum.

The amplitude and phase of the pulse in the time and frequency domains are shown in Figs. 4 and 5, respectively (solid lines). The pulse contains a nonlinear down-chirp, i.e., the blue components are present in the leading edge of the pulse and the red components in the trailing edge.

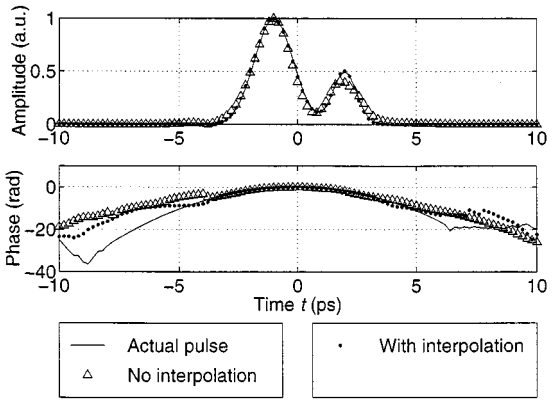

Fig. 4. Amplitude and phase of the nonlinearly chirped double pulse represented in the time domain: actual pulse (solid lines), reconstructed pulse using the TROG trace of Fig. 9 (triangles), and reconstructed pulse using the TROG trace of Fig. 10 (dots).

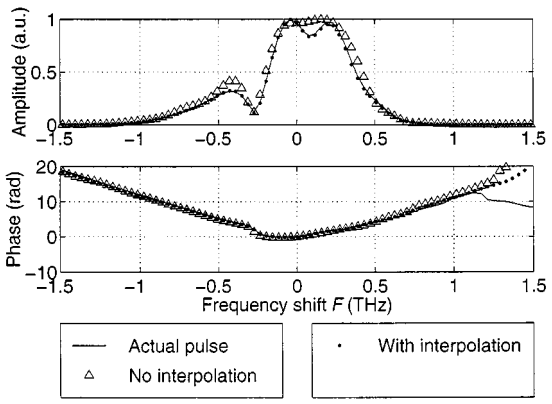

Fig. 5. Amplitude and phase of the nonlinearly chirped double pulse represented in the frequency domain: actual pulse (solid lines), reconstructed pulse using the TROG trace of Fig. 9 (triangles), and reconstructed pulse using the TROG trace of Fig. 10 (dots).

As a first step, the DP-TROG trace is calculated theoretically according to (17) and (18) on a $N \times N$ grid with $N = 128$. The time step taken is $\Delta T = 0.2\ t_0$ and the frequency step ΔF is given by (11). The number of points N and the time step ΔT need to be taken such that the total frequency range covered is large enough to contain the spectrum of the pulse and the total time range covered is large enough to contain the pulse shape for $D = 0$. The calculated DP-TROG trace is shown in Fig. 6. In order to show the low amplitude features of the trace, we have plotted its square root. Although the DP-TROG trace has certain ambiguities (see Appendix), it does not have an ambiguity in the direction of time in contrast to SHG-FROG where the direction of time for the pulse can not be distinguished [8]. The sign of the chirp is therefore directly revealed by the orientation of the trace in Fig. 6: the frequency decreases for increasing time, i.e., the pulse contains a down-chirp. The algorithm used to reconstruct the pulse from the DP-TROG trace is the basic method based on GP. On each iteration, the algorithm finds a new guess for the next iteration by minimizing (8) with respect to the real and imaginary parts of $\tilde{A}(f)$. The minimization method used is a $2N$-dimensional conjugate gradient method. We applied the standard Fletcher–Reeves minimization method [27], which involves a number of one-dimensional (1-D) minimizations along

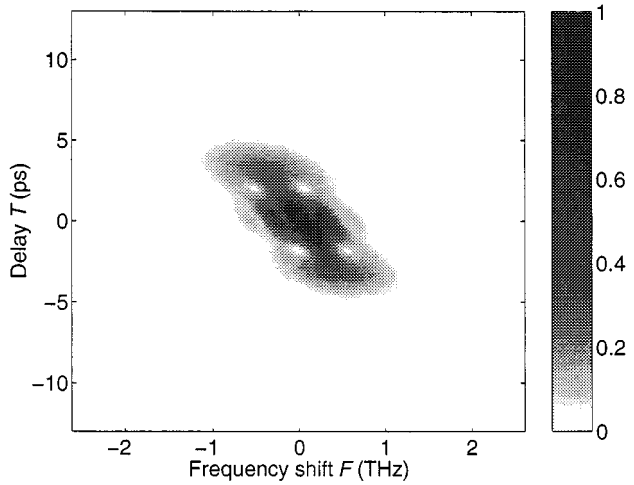

Fig. 6. DP-TROG trace generated from (17) and (18) for $N = 128$ and $\Delta T = 0.2t_0$.

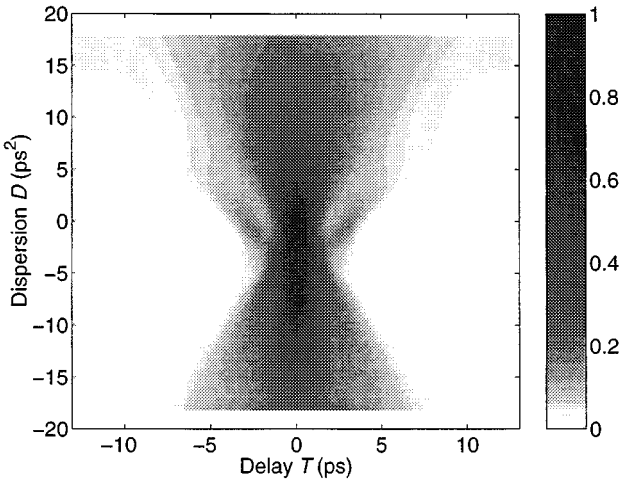

Fig. 7. Two-dimensional view of the set of autocorrelation traces $R(D, T)$ theoretically calculated from (13).

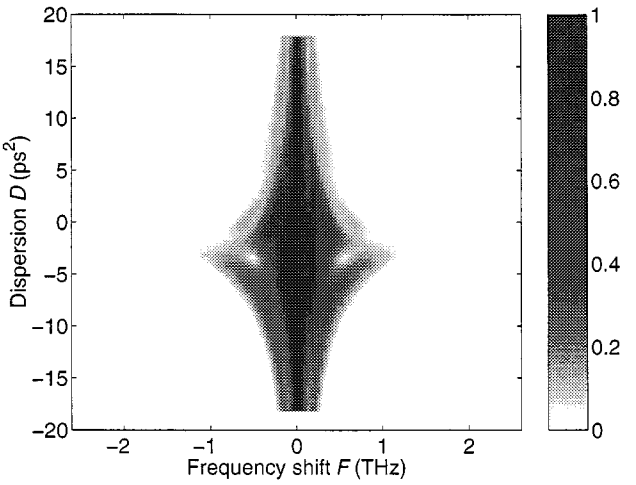

Fig. 8. Autocorrelation spectrum $\tilde{R}(D, F)$ obtained by Fourier transformation of the autocorrelation traces of Fig. 7 with respect to T.

directions that are selected with help of the gradient of $\hat{\epsilon}_{\mathrm{TROG}}$. Although the gradient with respect to the real and imaginary parts of $\tilde{A}(f)$ can be calculated numerically, the algorithm is sped up considerably by calculating an analytical expression for this gradient in a manner similar to that presented in [10]. One iteration takes approximately 1 s on a 200-MHz Pentium Pro. For the theoretically calculated TROG trace of Fig. 6, the algorithm converges to the exact pulse shape with a very small residual error $\hat{\epsilon}_{\mathrm{TROG}}$ on the order of 10^{-6}. For the initial guess, a random amplitude uniformly distributed on [0, 1] and a random phase uniformly distributed on $[-\pi, \pi]$ are chosen in the frequency domain.

As a next step, we have constructed the TROG trace from the autocorrelation measurements and the intensity spectrum of the dispersed pulse. The autocorrelation trace is calculated from (13) for different lengths of fiber. The dispersion parameter for regular fiber is taken as $\beta_2 = -23$ ps^2·km^{-1} while the step size in fiber length equals $\Delta L = 2$ m. The total dispersion is calculated according to $D = -2\pi\beta_2 L$. Negative total dispersion ($D < 0$) can be experimentally obtained by using dispersion compensating fiber ($\beta_2 > 0$). A 2-D view of the resulting set of autocorrelation traces is shown in Fig. 7. As expected, the pulse can be compressed with dispersion-compensating fiber due to its down-chirp. A minimum pulsewidth is achieved after propagation through $L = 12$ m of fiber. The spectrum $\tilde{R}(D, F)$ of the autocorrelation trace is obtained by Fourier transformation of the trace of Fig. 7 with respect to T. Its result is shown in Fig. 8.

The DP-TROG trace is now obtained by scaling the trace in Fig. 8 according to (19). As stated before, the trace with $F = 0$ cannot be acquired in this way but is replaced with the trace obtained by calculating (20). The result of this scaling is shown in Fig. 9. Looking at Fig. 9, there appears to be data missing in the TROG trace around $F = 0$. This is due to the limited range of dispersion D over which the autocorrelation trace is calculated. The area of missing data c+an be decreased by increasing the dispersion range over which the autocorrelation trace is calculated. This TROG trace is next used as input to the reconstruction algorithm. The time-domain constraint (7) is applied only on the areas of the TROG trace where data are present. The pulse reconstruction results after about 40 iterations are shown in Figs. 4 and 5 by the triangles. The final error is about $\epsilon_{\mathrm{TROG}} \approx 3 \times 10^{-3}$. It can be seen from Fig. 5 that, although there is a slight deviation in the intensity spectrum of the pulse, the algorithm reconstructs the spectral phase accurately. The mismatch in the intensity spectrum is caused by the limited dispersion range over which the autocorrelation traces are calculated. Running the algorithm on various pulse shapes and dispersion ranges, it is found that the spectral phase is always retrieved correctly while the mismatch in the intensity spectrum decreases if the dispersion range is increased. The dispersion range over which measurements should be made depends on the characteristics of the pulse that is being measured, but a good rule of thumb is as follows: find the amount of dispersion that compresses the pulse to its minimum autocorrelation width, then keep increasing the dispersion range around this dispersion amount until the measured autocorrelation trace has dropped its peak value to about one tenth of the peak value that would occur when the pulse is at its minimum autocorrelation width.

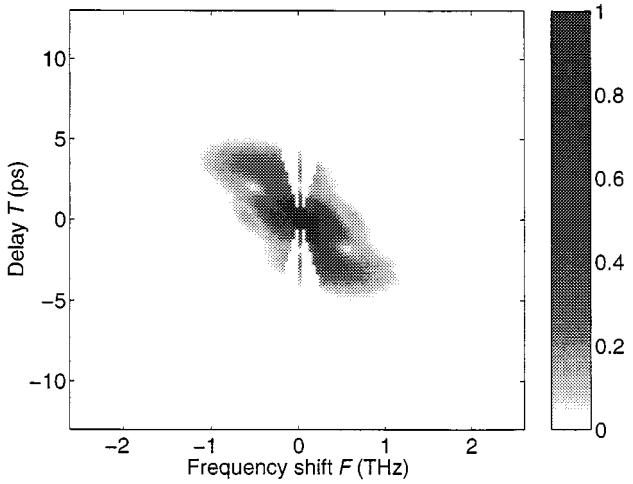

Fig. 9. Reconstructed DP-TROG trace obtained by scaling the autocorrelation spectrum of Fig. 8 in the T-direction according to (19) for $F \neq 0$. The trace for $F = 0$ is obtained from (20).

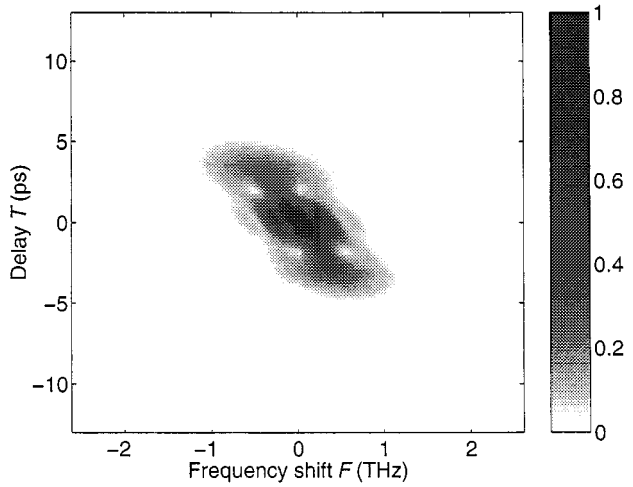

Fig. 10. Interpolated DP-TROG trace obtained by interpolating the trace of Fig. 9 in the F direction.

It is noted that a TROG trace contains redundant information: it is made up of $N \times N$ data points while the pulse shape is only determined by $2N$ points. One might thus try and exploit the two dimensions F and T of the trace to try to obtain TROG data around $F = 0$: we fill in the gaps of the TROG trace of Fig. 9 by doing N 1-D interpolations in the F direction. The resulting interpolated TROG trace is shown in Fig. 10. In order to find out the effects of this interpolation on the pulse reconstruction, we have again examined various pulse shapes and dispersion ranges. It is found that the algorithm convergence is approximately sped up by a factor of two, while the ability of the algorithm to retrieve the spectral phase is not affected. The ability to retrieve the correct spectral intensity is, however, strongly improved. To demonstrate this, we have run the algorithm on the final interpolated TROG trace of Fig. 10. Convergence occurs within 20 iterations and the final error is approximately $\epsilon_{\mathrm{TROG}} \approx 5 \times 10^{-4}$. The amplitude and phase of the retrieved pulse in the time and frequency domains are shown in Figs. 4 and 5, respectively, by the dots. Excellent pulse retrieval is accomplished.

As a final step, we have further tested the algorithm for the addition of multiplicative and additive noise to the autocorrelation trace. As TROG is similar to FROG except for the fact that the role of time and frequency is interchanged, noise reduction techniques that are available for FROG [12] can also be used for TROG. We have applied the techniques of mean background subtraction and median filtering to our noisy autocorrelation trace before running the reconstruction algorithm. For more details on these and other noise reduction procedures, the reader is referred to [12]. The algorithm retrieves the spectral phase very well for our test cases while the retrieved spectral intensity again slightly deviates from the actual one. It is noted that an accurate time-domain representation of the pulse can be obtained by using the spectral phase retrieved by the algorithm together with the measured intensity spectrum instead of the intensity spectrum retrieved by the algorithm. As an alternative, one can also add an intensity spectrum constraint to the algorithm. More details on noise reduction and other guidelines for experimentally obtained DP-TROG traces will be discussed in a separate paper [28].

V. Conclusion

We have introduced the TROG technique and shown its time–frequency duality with FROG. A new TROG geometry has been introduced based on DP. It has been shown that measurements of the autocorrelation traces of dispersed versions of the pulse together with a measurement of its spectrum are sufficient to recover phase and amplitude information. One of the advantages of the DP-TROG geometry is that it is simple to realize: it makes use of a dispersive medium and an autocorrelator. This equipment is usually already present in an optics laboratory. Although we use a set of fibers as the dispersive medium in our analysis, this might not be very practical in experiments as a large number of fibers is needed and their length will vary from experiment to experiment depending on the temporal width and chirp of the pulse. A grating or prism pulse stretcher/compressor is more appropriate as long as its dispersion can be adjusted below and above the value for which minimum autocorrelation width occurs and as long its optical loss is acceptable.

The DP-TROG geometry is a sensitive technique as it uses a second-order nonlinearity instead of a higher order one. It will work for any low-energy pulse that contains enough energy for the autocorrelation trace to be measured. We have also shown that this technique does not require a short gate pulse as is the case with FDPM-TROG. Compared with its frequency counterpart SHG-FROG, DP-TROG has two advantages. First, more sensitivity is obtained as there is no need to spectrally resolve the SHG signal. Second, the ambiguity in the direction of time, which is inherent in SHG-FROG, is not present in DP-TROG. SHG-FROG can, however, accurately retrieve the spectral intensity of the pulse without actually measuring it. In DP-TROG, a measurement of the intensity spectrum of the pulse is needed.

We have shown that the DP-TROG pulse reconstruction procedure works very well even for the case of a nonlinearly chirped double pulse and in the presence of multiplicative and additive noise: correct spectral phase reconstruction is

accomplished for all our test cases and algorithm convergence is sped up if the two-dimensionality of the TROG trace is exploited by means of interpolation. This also improves the retrieval of the correct spectral intensity.

It is expected that the DP-TROG method will be very useful, especially for characterizing pulses with low energy in the 1.3–1.5-μm wavelength range.

APPENDIX

The DP-TROG geometry has a number ambiguities. By an ambiguity, we mean that a certain change of the envelope $\tilde{A}(f)$ has no effect on the DP-TROG trace and the algorithm could thus converge to this solution. The following ambiguities are present and can be easily verified upon substitution together with (18) into (17):

1. A phase offset by φ_0

$$\tilde{A}(f) \rightarrow \tilde{A}(f)\exp(j\varphi_0). \tag{A1}$$

2. A shift in frequency by f_s

$$\tilde{A}(f) \rightarrow \tilde{A}(f - f_s). \tag{A2}$$

3. A mirror image of $\tilde{A}(f)$

$$\tilde{A}(f) \rightarrow \tilde{A}(-f). \tag{A3}$$

The first two ambiguities are trivial and of no concern in ultrashort pulse measurements as they represent a constant phase offset and an effective shift of the carrier frequency f_0. The third ambiguity would reverse the direction of time for the pulse upon inverse Fourier transformation. This ambiguity can easily be identified by comparing the reconstructed intensity spectrum with the measured one. If one is the mirror image of the other, the algorithm retrieved $\tilde{A}(-f)$ and $A(-t)$ and the pulse would have to be flipped in the time and frequency domains to obtain the correct one.

To find out whether there is an ambiguity in the direction of time, we calculate the TROG trace $I'_{\mathrm{DP-TROG}}(T, F)$ that results from the transformations

$$\tilde{A}(f) \rightarrow \tilde{A}^*(f) \tag{A4}$$

and

$$\tilde{A}(f) \rightarrow \tilde{A}^*(-f). \tag{A5}$$

The TROG trace for both transformation can be shown as

$$\begin{aligned} I'_{\mathrm{DP-TROG}}(T,F) &= I_{\mathrm{DP-TROG}}(-T,F) \\ &= I_{\mathrm{DP-TROG}}(T,-F) \end{aligned} \tag{A6}$$

where $I_{\mathrm{DP-TROG}}(T, F)$ is the TROG trace that would be obtained for $\tilde{A}(f)$. In the last equality, we have used the fact that the DP-TROG trace is centro-symmetric in T and F

$$I_{\mathrm{DP-TROG}}(T, F) = I_{\mathrm{DP-TROG}}(-T, -F) \tag{A7}$$

which can be easily verified.

The transformations of (A4) and (A5) thus lead to a TROG trace that is a flipped version in either the T or F direction of the TROG trace for $\tilde{A}(f)$. Due to the fact that these transformations lead to a different TROG trace, the algorithm will never converge to either $\tilde{A}^*(f)$ nor $\tilde{A}^*(-f)$ and the DP-TROG geometry has, therefore, no ambiguity in the direction of time for the pulse. It is noted that the SHG-FROG method contains this direction-of-time ambiguity due to the fact that the FROG trace is symmetric in the T direction and not in the F direction, i.e.,

$$I_{\mathrm{SHG-FROG}}(F, T) = I_{\mathrm{SHG-FROG}}(F, -T).$$

REFERENCES

[1] A. Yariv, *Optical Electronics in Modern Communications*, New York: Oxford University Press, 1997.

[2] K. L. Sala, G. A. Kenney-Wallace, and G. E. Hall, "CW autocorrelation measurements of picosecond laser pulses," *IEEE J. Quantum Electron.*, vol. 16, pp. 990–996, Sept. 1980.

[3] J. Peatross and A. Rundquist, "Temporal decorrelation of short laser pulses," *J. Opt. Soc. Amer. B*, vol. 15, no. 1, pp. 216–222, 1998.

[4] J. C. Diels, J. J. Fontaine, I. C. McMichael, and F. Simoni, "Control and measurement of ultrashort pulse shapes (in amplitude and phase) with femtosecond accuracy," *Appl. Opt.*, vol. 24, no. 9, pp. 1270–1282, 1985.

[5] K. Naganuma, K. Mogi, and H. Yamada, "General method for ultrashort light-pulse chirp measurement," *IEEE J. Quantum Electron.*, vol. 25, pp. 1225–1233, June 1989.

[6] C. Yan and J. C. Diels, "Amplitude and phase recording of ultrashort pulses," *J. Opt. Soc. Amer. B*, vol. 8, no. 6, pp. 1259–1263, 1991.

[7] C. Iaconis and I. A. Walmsley, "Spectral phase interferometry for direct electric-field reconstruction of ultrashort optical pulses," *Opt. Lett.*, vol. 23, no. 10, pp. 792–794, 1998.

[8] D. J. Kane and R. Trebino, "Characterization of arbitrary femtosecond pulses using frequency-resolved optical gating," *IEEE J. Quantum Electron.*, vol. 29, pp. 571–579, Feb. 1993.

[9] ——, "Single-shot measurement of the intensity and phase of an arbitrary ultrashort pulse by using frequency-resolved optical gating," *Opt. Lett.*, vol. 18, no. 10, pp. 823–825, 1993.

[10] K. W. DeLong and R. Trebino, "Improved ultrashort pulse-retrieval algorithm for frequency-resolved optical gating," *J. Opt. Soc. Amer. A*, vol. 11, no. 9, pp. 2429–2437, 1994.

[11] D. J. Kane, A. J. Taylor, R. Trebino, and K. W. DeLong, "Single-shot measurement of the intensity and phase of a femtosecond UV laser-pulse with frequency-resolved optical gating," *Opt. Lett.*, vol. 19, no. 14, pp. 1061–1063, 1994.

[12] D. N. Fittinghoff, K. W. DeLong, R. Trebino, and C. L. Ladera, "Noise sensitivity in frequency-resolved optical-gating measurements of ultrashort pulses," *J. Opt. Soc. Amer. B*, vol. 12, no. 10, pp. 1955–1967, 1995.

[13] K. W. DeLong, D. N. Fittinghoff, and R. Trebino, "Practical issues in ultrashort-laser-pulse measurement using frequency-resolved optical gating," *IEEE J. Quantum Electron.*, vol. 32, pp. 1253–1264, July 1996.

[14] K. W. DeLong, R. Trebino, and D. J. Kane, "Comparison of ultrashort-pulse frequency-resolved-optical-gating traces for 3 common beam geometries," *J. Opt. Soc. Amer. B*, vol. 11, no. 9, pp. 1595–1608, 1994.

[15] J. R. Fienup, "Phase retrieval algorithms—A comparison," *Appl. Opt.*, vol. 21, no. 15, pp. 2758–2769, 1982.

[16] R. Trebino and D. J. Kane, "Using phase retrieval to measure the intensity and phase of ultrashort pulses-frequency-resolved optical gating," *J. Opt. Soc. Amer. A*, vol. 10, no. 5, pp. 1101–1111, 1993.

[17] K. W. DeLong, R. Trebino, J. Hunter, and W. E. White, "Frequency-resolved optical gating with the use of second-harmonic generation," *J. Opt. Soc. Amer. B*, vol. 11, no. 11, pp. 2206–2215, 1994.

[18] K. W. DeLong, D. N. Fittinghoff, R. Trebino, B. Kohler, and K. Wilson, "Pulse retrieval in frequency-resolved optical gating based on the method of generalized projections," *Opt. Lett.*, vol. 19, no. 24, pp. 2152–2154, 1994.

[19] D. J. Kane, G. Rodriguez, A. J. Taylor, and T. S. Clement, "Simultaneous measurement of two ultrashort laser pulses from a single spectrogram in a single shot," *J. Opt. Soc. Amer. B*, vol. 14, no. 4, pp. 935–943, 1997.

[20] D. J. Kane, "Real-time measurement of ultrashort laser pulses using principal component generalized projections," *IEEE J. Select. Topics Quantum Electron.*, vol. 4, pp. 278–284, 1998.

[21] J. L. A. Chilla and O. E. Martinez, "Direct determination of the amplitude and the phase of femtosecond light-pulses," *Opt. Lett.*, vol. 16, no. 1, pp. 39–41, 1991.

[22] ——, "Analysis of a method of phase measurement of ultrashort pulses in the frequency-domain," *IEEE J. Quantum Electron.*, vol. 27, pp. 1228–1235, May 1991.
[23] ——, "Frequency-domain phase measurement of ultrashort light-pulses-effect of noise," *Opt. Commun.*, vol. 89, no. 5-6, pp. 434–440, 1992.
[24] V. Wong and I. A. Walmsley, "Ultrashort-pulse characterization from dynamic spectrograms by iterative phase retrieval," *J. Opt. Soc. Amer. B*, vol. 14, no. 4, pp. 944–949, 1997.
[25] O. E. Martinez, "3000 times grating compressor with positive group-velocity dispersion-application to fiber compensation in 1.3–1.6 μm region," *IEEE J. Quantum Electron.*, vol. 23, pp. 59–64, Jan. 1987.
[26] R. L. Fork, O. E. Martinez, and J. P. Gordon, "Negative dispersion using pairs of prisms," *Opt. Lett.*, vol. 9, no. 5, pp. 150–152, 1984.
[27] W. H. Press, S. A. Teukolsky, W. T. Vetterling, and B. P. Flannery, *Numerical Recipes in C*. New York, NY: Cambridge University Press, 1992.
[28] R. G. M. P. Koumans and A. Yariv. "Pulse characterization at 1.5 μm using time-resolved optical gating based on dispersive propagation," unpublished.

Roger G. M. P. Koumans was born in Heerlen, The Netherlands, on January 17, 1971. He received the B.S. and the M.S. degrees *(cum laude)* in electrical engineering from Eindhoven University of Technology, Division of Optical Telecommunications, Eindhoven, The Netherlands, in June 1994. Since September 1995, he has been working toward the Ph.D. degree at the California Institute of Technology, Pasadena.

During 1994, he worked for Philips Optoelectronics Centre, Eindhoven, on mode-locked lasers in partial fulfillment of the M.S. degree. He continued to work with the Division of Optical Telecommunications in Eindhoven on the subject of cross-talk in multiwavelength optical network interconnects for a year. His research interests are mode locking in semiconductor and fiber lasers and its applications, wavelength division multiplexing, ultrashort pulse measurements and pulse shaping, wavelength conversion, fiber gratings, and nonlinear optics.

Amnon Yariv (S'56–M'59–F'70–LF'95) is a native of Tel Aviv, Israel. He obtained the B.S., M.S., and Ph.D. degrees in electrical engineering from the University of California in Berkeley in 1954, 1956, and 1958, respectively.

He went to the Bell Telephone Laboratories, Murray Hill, NJ, in 1959, joining the early stages of the laser effort. He came to the California Institute of Technology, Pasadena, in 1964 as an Associate Professor of Electrical Engineering, becoming a Professor in 1966. In 1980, he became the Thomas G. Myers Professor of Electrical Engineering and in 1996, he became the Martin and Eileen Summerfield Professor of applied physics. On the technical side, he took part in the discovery of a number of early solid-state laser systems, in proposing and demonstrating the field of semiconductor integrated optics, the invention of the semiconductor distributed feedback laser, and in pioneering the field of phase conjugate optics. He has published widely in the laser and optics fields and has written a number of basic texts in quantum electronics, optics, and quantum mechanics.

Dr. Yariv is a member of the American Physical Society, Phi Beta Kappa, the American Academies of Arts and Sciences, the National Academies of Engineering and Sciences, and a fellow of the Optical Society of America (OSA). He has received the 1980 Quantum Electronics Award of the IEEE, the 1985 University of Pennsylvania Pender Award, the 1986 OSA Ives Medal, the 1992 Harvey Prize, and the 1998 OSA Beller Award.